

A Flux-Based Estimate of the Interstellar Object Contribution to the Galactic Baryon Budget

Marian Siwiak¹

Cognition Shared Solutions LLC, 16192, Lewes, USA
e-mail: marian.siwia@cognition.llc

Received November 20, 2025

ABSTRACT

Context. Interstellar objects provide the only direct observational evidence for macroscopic bodies unbound to the Solar System. Their potential contribution to the Galactic baryon budget has not previously been quantified using an observation-anchored approach.

Aims. We aim to determine whether the population implied by the three confirmed interstellar objects can supply a significant fraction of the Milky Way’s missing baryons.

Methods. We derive a flux-based estimate of the local ISO number density using measured detection radii, encounter times, and hyperbolic velocities, and convert this to a local mass density via a non-parametric bootstrap over the ISO masses. This density is then coupled to several Galactic spatial templates and integrated across the Milky Way to obtain the corresponding Galaxy-wide ISO mass. Detection completeness is treated as a free scaling parameter, and Poisson and mass uncertainties are propagated independently.

Results. For the three shallow-gradient templates considered—baryonic, total-mass, and uniform—modest incompleteness is sufficient for ISOs to supply the mass needed to raise the Milky Way baryon fraction to the value expected for haloes of similar mass. Stronger incompleteness allows the inferred baryon fraction to approach the cosmic value. A stellar-tracing template yields unphysical Galaxy-wide masses and is therefore ruled out.

Conclusions. Interstellar objects may constitute a non-negligible and previously unaccounted component of the Galactic baryon budget. The framework developed here is readily updated as additional ISOs are detected, providing a direct and observation-anchored means of assessing their contribution to the Milky Way’s baryonic mass.

Key words. ISM: general – Galaxies: ISM – Galaxy: structure – Galaxy: fundamental parameters – Methods: statistical – Methods: numerical

1. Introduction

The baryonic mass of the Milky Way remains uncertain. Measurements from the cosmic microwave background and big-bang nucleosynthesis constrain the cosmic baryon fraction to $f_b \simeq 0.158$ (Aghanim et al. 2020; Fields et al. 2020), whereas dynamical estimates for the Galaxy indicate a substantially smaller value, $f_b \simeq 0.05\text{--}0.06$ (McMillan 2017; Bland-Hawthorn & Gerhard 2016). This difference implies a missing baryonic mass of order $2\text{--}3 \times 10^{10} M_\odot$, potentially residing in hot circumgalactic gas, cold or diffuse phases, or compact baryonic components (Bregman 2007; Tumlinson et al. 2017; Priyadharshini et al. 2025).

Interstellar objects (ISOs) constitute a rarely examined category within this broader inventory. Prior to the discovery of 1I/’Oumuamua, constraints relied solely on survey non-detections (Engelhardt et al. 2017). The subsequent detections of 1I/’Oumuamua, 2I/Borisov, and 3I/ATLAS (Meech et al. 2017; Guzik et al. 2020; Seligman et al. 2025) provide direct evidence for macroscopic bodies on unbound trajectories through the Solar System and allow a flux-based estimate of their local number density (Flekkøy & Toussaint 2023; Dorsey et al. 2025). Because ISOs originate from baryonic processes associated with planet formation and early dynamical ejection (Jackson et al. 2018; Raymond et al. 2018), they represent a potentially non-negligible but previously unquantified baryonic reservoir.

In this paper we use only the empirical properties of the three known ISOs—detection radii, encounter times, heliocentric ve-

locities, and estimated masses—to derive the corresponding local number and mass densities. We propagate these constraints through a set of conservative Galactic-scale spatial templates and integrate the resulting ISO density fields across the Milky Way. This approach quantifies how the Galaxy-wide ISO mass depends on survey completeness while avoiding assumptions about the underlying mass function or ejection history.

The analysis shows that, for spatial distributions tracing baryonic mass, total mass, or a uniform background, modest incompleteness is sufficient for ISOs to supply a baryonic mass comparable to the present deficit. More extreme incompleteness values allow the ISO contribution to approach the baryon fraction empirically associated with haloes of Milky-Way mass. A stellar-tracing template, in contrast, produces unphysical Galaxy-wide masses and is therefore excluded. ISOs cannot serve as a dark-matter analogue, both because of their baryonic origin and because such an interpretation would conflict with cosmological constraints; however, they may form a previously unaccounted component of the Galactic baryon budget.

All analysis code and figure-generation scripts are publicly available at <https://github.com/mariansiwiak/ISODensity>.

2. Modelling

The three confirmed interstellar objects—1I/Oumuamua, 2I/Borisov, and 3I/ATLAS—provide the empirical foundation for estimating the local ISO mass density and extrapolating it to the Galaxy. Their discovery circumstances (Meech et al. 2017; Guzik et al. 2020; Seligman et al. 2025) and associated photometric and dynamical characterisation (Jewitt et al. 2017, 2020; Jewitt 2024; Bolin et al. 2020) supply the observed encounter dates t_i , heliocentric detection radii R_i , estimated masses m_i , and characteristic hyperbolic velocities v_∞ (Table 1). These observational inputs, together with survey sensitivity considerations (Engelhardt et al. 2017; Chambers et al. 2019; Tonry et al. 2018), define the local normalisation used in the remainder of the analysis.

Table 1: Adopted parameters for the three confirmed interstellar objects.

Object	Discovery date	R_{det} (AU)	Mass (kg)	v_∞ (km s ⁻¹)
1I	19/10/17	0.25	1.0×10^{11a}	26.3^b
2I	30/08/19	2.98	2.6×10^{11c}	32^d
3I	01/07/25	3.20	2.6×10^{14e}	58^f

Notes. ^(a) Jewitt (2024) ^(b) NASA Science (2017) ^(c) Jewitt et al. (2020) ^(d) Bolin et al. (2020) ^(e) Seligman et al. (2025) ^(f) NASA Science (2025)

2.1. Local ISO encounter rate and number density

The temporal baseline between the first and last detection is

$$T_{\text{obs}} = t_{\text{max}} - t_{\text{min}}, \quad (1)$$

yielding the maximum-likelihood Poisson arrival rate

$$\lambda_{\text{best}} = \frac{N_{\text{det}}}{T_{\text{obs}}}. \quad (2)$$

Uncertainty in the rate is quantified using the exact Garwood interval (Garwood 1936), which provides the 95% bounds ($\lambda_{\text{low}}, \lambda_{\text{high}}$), expressed through the multiplicative factors

$$s_{\text{low}} = \frac{\lambda_{\text{low}}}{\lambda_{\text{best}}}, \quad s_{\text{high}} = \frac{\lambda_{\text{high}}}{\lambda_{\text{best}}}. \quad (3)$$

Because the three ISOs were detected at different heliocentric distances and no uniform survey-sensitivity model exists for all events, we adopt the arithmetic mean

$$R_{\text{avg}} = \frac{1}{N_{\text{det}}} \sum_i R_i, \quad (4)$$

and treat the surveyed region as an effective sphere of cross-section

$$A = \pi R_{\text{avg}}^2. \quad (5)$$

This choice provides a conservative, survey-independent normalisation. The corresponding flux-through-a-sphere formulation for the local ISO density follows the standard approach used in recent ISO visibility and number-density analyses (Flekkøy & Toussaint 2023; Dorsey et al. 2025).

Equating the flux $n_{\text{ISO}} v_\infty A$ to the observed arrival rate gives the local number-density estimator

$$n_{\text{ISO}} = \frac{\lambda_{\text{best}}}{A v_\infty}. \quad (6)$$

In this work, the detection completeness factor $C_{\text{det}} \in (0, 1]$ is introduced as a free scaling parameter to probe the sensitivity of the inferred ISO mass to survey incompleteness. C_{det} rescales flux calculated in equation 6 to

$$n_{\text{ISO,true}}(C_{\text{det}}) = \frac{n_{\text{ISO}}}{C_{\text{det}}} = \frac{\lambda}{C_{\text{det}} A v_\infty}. \quad (7)$$

2.2. Local ISO mass density and normalisation

The estimated masses of the three ISOs span several orders of magnitude, consistent with expectations from population synthesis and ejection models (Jackson et al. 2018; Raymond et al. 2018; Trilling et al. 2017; Portegies Zwart et al. 2018). To avoid imposing a parametric mass distribution, we employ a non-parametric bootstrap (Efron 1979; Feigelson & Babu 2012) over the mass set $\{m_1, m_2, m_3\}$. This generates an empirical distribution of mean masses and yields the low, best, and high estimates $m_{\text{avg,low}}, m_{\text{avg,best}}, m_{\text{avg,high}}$. The corresponding local mass density is

$$\rho_{\text{ISO,true}}(C_{\text{det}}) = m_{\text{avg}} n_{\text{ISO,true}}(C_{\text{det}}) = \frac{m_{\text{avg}} \lambda}{C_{\text{det}} A v_\infty}. \quad (8)$$

2.3. Galaxy-wide ISO mass extrapolation

To extrapolate the local mass density to the Galaxy, we assume that the ISO spatial distribution follows one of four templates: stellar mass, total baryonic mass, total mass (baryons + dark matter), or a uniform background. These distributions are derived from the Milky Way mass model of McMillan (2017) as implemented in galpy (Bovy 2015). For any template $\rho_T(R, z)$, the ISO density normalised at the Solar position (R_\odot, z_\odot) = (8.2 kpc, 0) (Abuter et al. 2019) is

$$\rho_{\text{ISO}}(R, z; C_{\text{det}}) = \rho_{\text{ISO}}(C_{\text{det}}) \frac{\rho_T(R, z)}{\rho_T(R_\odot, 0)}. \quad (9)$$

We evaluate the distribution on an axisymmetric cylindrical grid spanning $R \in [0.1, 20]$ kpc and $z \in [-3, 3]$ kpc, using the volume element $dV = 2\pi R dR dz$. The total ISO mass is approximated by

$$M_{\text{ISO}}(C_{\text{det}}) \approx \sum_{i,j} \rho_{\text{ISO}}(R_i, z_j; C_{\text{det}}) (2\pi R_i \Delta R_i \Delta z_j), \quad (10)$$

and the corresponding baryon fraction is

$$f_b(C_{\text{det}}) = \frac{M_{\text{bary,known}} + M_{\text{ISO}}(C_{\text{det}})}{M_{\text{total}}}. \quad (11)$$

All unit conversions are handled through the ASTROPY framework (Collaboration 2022).

2.4. Uncertainty treatment

Two independent sources of uncertainty enter the model: the Poisson arrival rate and the ISO masses. Rate uncertainty is captured through the Garwood scalings ($s_{\text{low}}, s_{\text{high}}$) applied to λ_{best} . Mass uncertainty is captured through the bootstrap-derived

triplet ($m_{\text{avg,low}}, m_{\text{avg,best}}, m_{\text{avg,high}}$). These are propagated independently through the number-density calculation, the local mass density, and the Galactic integration.

The combined uncertainty envelope is therefore obtained by applying all combinations of the three mass scenarios, and the two rate scalings, explicitly:

$$\rho_{\text{ISO,true}}^{\text{comb}} = \rho_{\text{ISO,true}}^{\text{best}} \times \{s_{\text{low}}, s_{\text{high}}\} \times \left\{ \frac{m_{\text{avg,low}}}{m_{\text{avg,best}}}, \frac{m_{\text{avg,high}}}{m_{\text{avg,best}}} \right\}. \quad (12)$$

These cases are propagated independently through the Galactic integration, producing the full uncertainty envelope for the total ISO mass $M_{\text{ISO}}(C_{\text{det}})$ and the baryon fraction $f_b(C_{\text{det}})$.

3. Results

Galaxy-integrated ISO masses increase monotonically as the detection completeness C_{det} decreases, and this trend directly shapes the inferred baryon fraction. As shown in Fig. 1, the three shallow-gradient templates (baryonic, total-mass, and uniform) produce nearly identical trends across the detection completeness range, whereas the stellar template deviates by several orders of magnitude.

value ($f_b \simeq 0.056$), the halo-mass-expected value ($f_b \simeq 0.08$; McGaugh 2007; McGaugh et al. 2009; Priyadharshini et al. 2025), and the cosmic value ($f_b = 0.158$; Aghanim et al. 2020; Fields et al. 2020)—are summarised in Table 2.

Table 2: Completeness values C_{det} at which each template reaches selected baryon-fraction thresholds.

Template (f_b)	0.056	0.08	0.158	1
Stellar	1.0	1.0	1.0	1.0
Baryonic	1.0	0.46	0.10–0.31	0.01–0.03
Total-mass	1.0	0.39–1.0	0.09–0.27	0.03
Uniform	1.0	0.33–1.0	0.08–0.23	0.02–0.03

Across the viable models, modest incompleteness is sufficient to reach $f_b \simeq 0.08$, while stronger incompleteness allows f_b to approach the cosmic value.

3.2. Behaviour across the shallow-gradient templates

Figure 1 shows that the inferred ISO contribution increases monotonically with decreasing C_{det} . This trend follows directly from the C_{det}^{-1} scaling of the local mass density. Even for $C_{\text{det}} = 1$, ISOs contribute at the several-percent level to the Milky Way baryonic mass.

The three viable spatial templates are compared more closely in Figure 2. Each panel displays the best-estimate curve together with the uncertainty envelopes derived from the bootstrap mass distribution and Poisson rate bounds. The similarity of the three panels shows that the results are driven primarily by the local ISO normalisation and only weakly by assumptions about the large-scale spatial distribution.

3.3. Implications for the missing-baryon budget

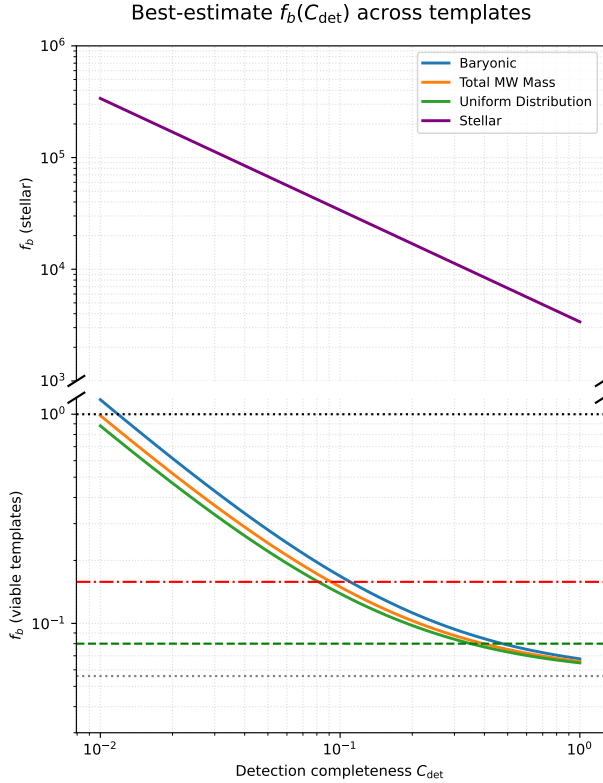
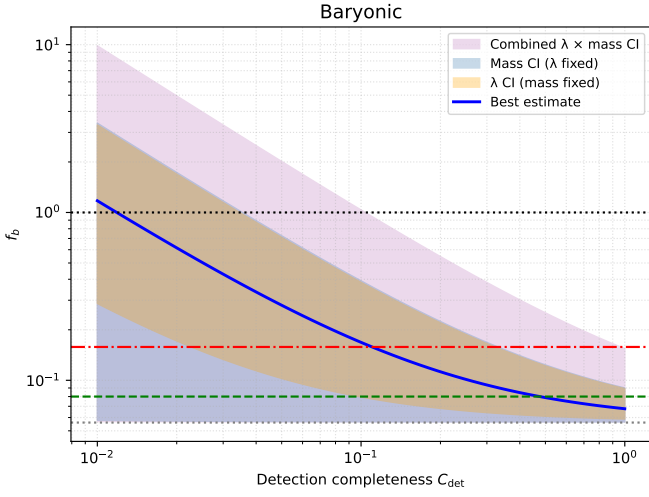


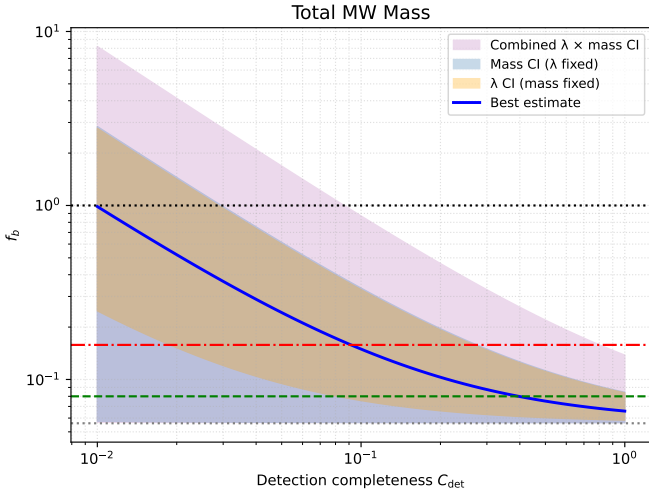
Fig. 1: Best-estimate $f_b(C_{\text{det}})$ across the galactic templates. Horizontal lines mark the Milky Way baryon fraction, the expected fraction for haloes of similar mass, and the cosmic baryon fraction.

3.1. Crossing points for characteristic baryon fractions

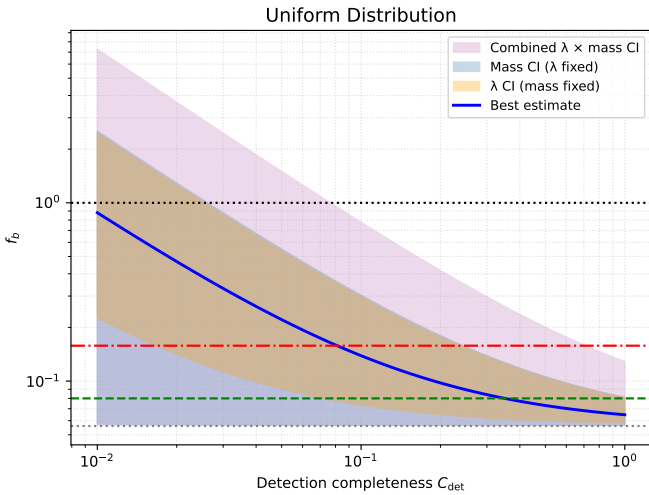
The completeness values at which the inferred baryon fraction reaches three characteristic thresholds—the Milky Way



(a) Baryonic template



(b) Total-mass template



(c) Uniform template

Fig. 2: Uncertainty envelopes for the three shallow-gradient templates. The three panels show nearly identical behaviour across the completeness range.

The gap between the Milky Way baryon fraction and the value expected for haloes of comparable mass corresponds to roughly $(2-3) \times 10^{10} M_{\odot}$. As shown in Figure 1, once the completeness falls below $C_{\text{det}} \lesssim 0.6$, the inferred ISO contribution exceeds this threshold for all viable templates. For $C_{\text{det}} \approx 0.1-0.15$, the corresponding baryon fractions approach the cosmic value. These trends follow directly from the local ISO normalisation implied by the detections and arise without invoking changes to the underlying Galactic mass model.

3.4. Stellar-tracing template

The stellar template behaves qualitatively differently due to the steep central concentration of the stellar density field (McMillan 2017). When normalised to the Solar neighbourhood, this leads to Galaxy-integrated ISO masses that exceed both the baryonic and dynamical mass of the Milky Way. Even the most conservative uncertainty combinations give $f_b \gg 1$, as shown in Fig. 3.

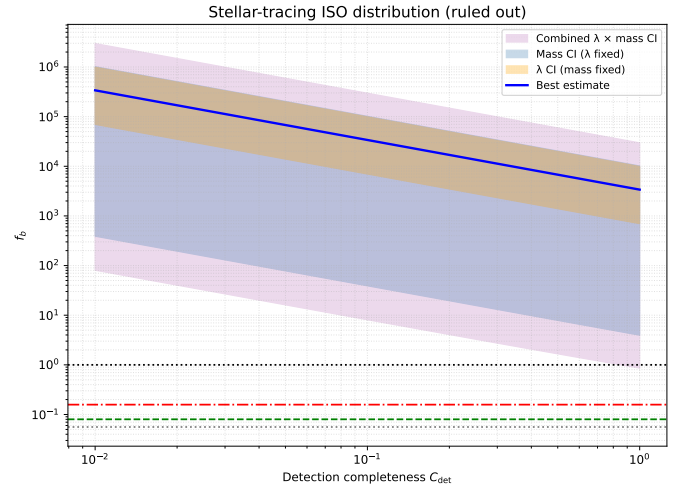


Fig. 3: Stellar-tracing template. The inferred baryon fraction exceeds unity for all completeness values, indicating incompatibility with the ISO normalisation.

4. Conclusions

We have developed a minimal, observation-anchored framework for estimating the possible Galactic mass contribution of interstellar objects, based solely on the measured properties of the three confirmed detections. A flux-based estimate of the local ISO number density, combined with a bootstrap characterisation of ISO masses and an exact Poisson description of the arrival rate, provides a data-driven normalisation for several conservative Galactic density templates derived from the McMillan mass model.

The three shallow-gradient templates—baryonic, total-mass, and uniform—produce mutually consistent outcomes. For completeness values $C_{\text{det}} \lesssim 0.6$, the corresponding Galaxy-integrated ISO masses are sufficient to raise the Milky Way baryon fraction from its currently inferred value to the $f_b \approx 0.08$ level expected for haloes of comparable mass. For $C_{\text{det}} \approx 0.1-0.15$, the inferred fractions extend toward the cosmic baryon fraction. These behaviours are driven by the local ISO density and are largely insensitive to the assumed large-scale spatial distribution.

The stellar-tracing template yields baryon fractions well above unity owing to the steep central concentration of the stellar mass field. This incompatibility with the observed ISO environment provides an internal consistency check on the modelling framework and motivates the exclusion of such centrally concentrated distributions.

Low completeness values allow the inferred ISO mass to approach the dynamical mass scale of the Galaxy. Under the standard cosmological baryon inventory, this trend cannot be interpreted as evidence for a baryonic alternative to dark matter: ISO formation is inherently baryonic, and any associated increase in f_b would need to remain consistent with CMB- and BBN-based constraints. Within those constraints, the results should be viewed in terms of Galactic baryon accounting; should future revisions of the cosmological baryon fraction arise, the ISO component quantified here would integrate naturally into any updated budget.

The framework is readily extensible. Additional ISO detections will tighten the arrival-rate constraints, reduce statistical uncertainty, and progressively constrain the ISO mass distribution. Improvements in survey sensitivity models, ISO physical characterisation, and Galactic potential modelling can be incorporated directly. As the sample grows, this approach provides a stable means of quantifying the role of interstellar objects in the Milky Way baryon census, complementing ongoing efforts to identify and characterise non-luminous baryonic components.

References

- Abuter, R., Amorim, A., et al. 2019, *Astronomy & Astrophysics*, 625, L10
Aghanim, N. et al. 2020, *Astronomy and Astrophysics*, 641, A6
Bland-Hawthorn, J. & Gerhard, O. 2016, *Annual Review of Astronomy and Astrophysics*, 54, 529
Bolin, B. T. et al. 2020, *The Astronomical Journal*, 159, 107
Bovy, J. 2015, *The Astrophysical Journal Supplement Series*, 216, 29
Bregman, J. N. 2007, *Annual Review of Astronomy and Astrophysics*, 45, 221
Chambers, K. C. et al. 2019, arXiv preprint
Collaboration, A. 2022, *The Astrophysical Journal*, 935, 167
Dorsey, R. C., Bannister, M. T., et al. 2025, *The Planetary Science Journal*, 6, 214
Efron, B. 1979, *Annals of Statistics*, 7, 1
Engelhardt, T., Jedicke, R., Vereš, P., et al. 2017, *The Astronomical Journal*, 153, 133
Feigelson, E. D. & Babu, G. J. 2012, *Modern Statistical Methods for Astronomy: With R Applications* (Cambridge University Press)
Fields, B. D., Olive, K. A., & Yeh, T.-H. 2020, *Journal of Cosmology and Astroparticle Physics*, 2020, 010
Flekkøy, E. G. & Toussaint, R. 2023, *Monthly Notices of the Royal Astronomical Society: Letters*, 523, L9
Garwood, F. 1936, *Biometrika*, 28, 437
Guzik, P. et al. 2020, *Nature Astronomy*, 4, 53
Jackson, A. P., Tamayo, D., Hammond, N., Ali-Dib, M., & Rein, H. 2018, *Monthly Notices of the Royal Astronomical Society: Letters*, 478, L49
Jewitt, D. 2024, arXiv preprint
Jewitt, D., Weaver, H., Mutchler, M., Larson, S., & Agarwal, J. 2017, *The Astrophysical Journal Letters*, 850, L36
Jewitt, D. et al. 2020, *The Astrophysical Journal Letters*, 888, L23
McGaugh, S. S. 2007, *Proceedings of the International Astronomical Union*, 3, 136
McGaugh, S. S., Schombert, J. M., de Blok, W. J. G., & Zgursky, M. J. 2009, *The Astrophysical Journal Letters*, 708, L14, publisher: The American Astronomical Society
McMillan, P. J. 2017, *Monthly Notices of the Royal Astronomical Society*, 465, 76
Meech, K. J. et al. 2017, *Nature*, 552, 378
NASA Science. 2017, ‘Oumuamua — What We Know
NASA Science. 2025, As NASA Missions Study Interstellar Comet, Hubble Makes Size Estimate
Portegies Zwart, S., Torres, S., Pelupessy, I., & Bédorf, J. 2018, *Monthly Notices of the Royal Astronomical Society: Letters*, 479, L17
Priyadharshini, V., Vijikumar, S., & Bhuvaneshwari, V. 2025, *Theoretical and Mathematical Physics*, 223, 879

- Raymond, S. N., Armitage, P. J., & Veras, D. 2018, *Monthly Notices of the Royal Astronomical Society*, 476, 3031
Seligman, D. Z., Micheli, M., Farnocchia, D., et al. 2025, *The Astrophysical Journal Letters*, 989, L36
Tonry, J. L. et al. 2018, *Publications of the Astronomical Society of the Pacific*, 130, 064505
Trilling, D. E. et al. 2017, *The Astrophysical Journal Letters*, 850, L38
Tumlinson, J., Peebles, M. S., & Werk, J. K. 2017, *Annual Review of Astronomy and Astrophysics*, 55, 389

270